PHOTOSYNTHETICA
International Journal for Photosynthesis Research

DOI 10.32615/ps.2024.040 PHOTOSYNTHETICA 62 (4): 372-380, 2024

Using hyperspectral reflectance to detect changes in photosynthetic activity in *Atractylodes chinensis* leaves as a function of decreasing soil water content

J. LIU[*], Y. WANG[**], X.M. LIN[***], Z.C. XUE[**,+], and F.R. ZENG[#]

College of Teacher Education, Hebei Minzu Normal University, 067000 Chengde, Hebei, China[*]
School of Resources and Environmental Sciences, Innovative Research Center for Soil and Plant Nutrition in Mountain Areas of Northern Hebei, Hebei Minzu Normal University, 067000 Chengde, Hebei, China[**]
Laboratory Management Center, Hebei Minzu Normal University, 067000 Chengde, Hebei, China[***]
Chengde Bijiashan Ecological Agriculture Technology Development Co., Ltd., 067000 Chengde, Hebei, China[#]

Abstract

Application of hyperspectral reflectance technology to track changes in photosynthetic activity in *Atractylodes chinensis* (*A. chinensis*) remains underexplored. This study aimed to investigate the relationship between hyperspectral reflectance and photosynthetic activity in the leaves of *A. chinensis* in response to a decrease in soil water content. Results demonstrated that the reflectance in both the visible light and near-infrared bands increased in conjunction with reduced soil water content. The derived vegetable indices of photochemical reflection index (PRI) and the pigment-specific simple ratio of chlorophyll *b* ($PSSR_b$) gradually decreased. In contrast, the normalized difference in water index (NWI) and water index (WI) increased. Moreover, significant correlations were observed between PRI, $PSSR_b$, WI, and NWI and photosynthetic activity indices, namely photosynthetic rate and total performance index. Consequently, hyperspectral reflection represents a productive approach for evaluating the influence of water deficit on photosynthetic activity in *A. chinensis* leaves.

Keywords: *Atractylodes chinensis*; hyperspectral reflectance; photosynthesis; vegetable indices; water stress.

Highlights

- Photosynthetic activity in *Atractylodes chinensis* leaves is altered under water stress
- Spectral reflectance in *A. chinensis* leaves increased with decreasing soil water content
- Spectral reflectance allows the detection of photosynthetic activity changes in *A. chinensis* leaves

Received 11 June 2024
Accepted 12 November 2024
Published online 5 December 2024

[+]Corresponding author
e-mail: zhongcaix2023@hbun.edu.cn

Abbreviations: ABS/RC – absorption flux per RC; Chl – chlorophyll; C_i – intercellular CO_2 concentration; CTG – control group; DI_0/RC – dissipated energy flux per RC at t = 0; *E* – transpiration rate; ET_0/RC – electron transport flux per RC at t = 0; F_t – fluorescence emission from a dark-adapted leaf at the time t; g_s – stomatal conductance; M_0 – slope of the curve at the origin of the relative variable fluorescence rise; MCG – water consumption group; NWI – normalized difference water index; PI_{ABS} – performance index; PI_{total} – the total performance index; P_N – net photosynthetic rate; PRI – photochemical reflection index; $PSSR_a$ – pigment specific simple ratio of Chl *a*; $PSSR_b$ – pigment specific simple ratio of Chl *b*; RC – reaction center; RC/CS_0 – Q_A^- reducing RCs per CS; RE_0/RC – electron flux per active RC reducing the end electron acceptors on the acceptor side of PSI at t = 0; ROS – reactive oxygen species; TR_0/RC – trapped energy flux per RC at t = 0; WI – water index; WUE – water-use efficiency; δ_{R0} – probability that an electron is transported from the reduced intersystem electron acceptors to the final electron acceptors of PSI; φ_{P0} – maximum quantum yield for primary photochemistry; ψ_{E0} – probability that an electron moves further than Q_A^-.

Acknowledgments: We are grateful to the Central Guidance for Local Science and Technology Development Fund Project of Hebei Province (No. 246Z6403G), the Huizhilingchuang Space Project of Hebei Minzu Normal University (No. HZLC2024016) for their financial support of this study.

Conflict of interest: The authors declare that they have no conflict of interest.

Introduction

Atractylodes chinensis (DC.) Koidz. (*A. chinensis*), is a perennial herb (Xia *et al.* 2013); its dry rhizome is one of the important basic sources of traditional Chinese medicine *Atractylodis rhizoma* (Zhang *et al.* 2021a, 2023), which is rich in semiterpenes, sesquiterpenes, alkynes, sterols, and polysaccharides (Lei *et al.* 2023, Ma *et al.* 2023), mainly for abdominal distension, diarrhea, edema, rheumatism, indigestion, and other diseases (Xu *et al.* 2016). It also plays an important role in treating and preventing novel coronavirus (COVID-19) (Lei *et al.* 2022). In addition, the area under cultivation of *A. chinensis* is expanding in response to the shortage of wild resources and increasing market demand.

Water, one of the most important substances for maintaining plant life activities and growth metabolism, plays an important role in plant growth and development, yield, and quality formation (Gupta *et al.* 2020, Ilyas *et al.* 2021). Our previous studies have shown that precipitation is one of the main factors controlling the habitat distribution of *A. chinensis* in the Yanshan district of north Hebei (Wang *et al.* 2023). It corroborates the previous view that variations in soil moisture can lead to changes in gene expression in *A. chinensis* (Ma *et al.* 2024). Moreover, moderate drought promotes the formation and accumulation of pharmacodynamic substances, such as atractylodes, atractylodes ketone, and β-cineole in *A. chinensis*. Severe drought negatively impacts its growth and quality (Zhang *et al.* 2021b). However, soil water deficiency leads to water loss in plant leaves, resulting in decreased photosynthesis, thus inhibiting the growth of plants (Gupta *et al.* 2020). Therefore, monitoring the change in photosynthesis of plant leaves is an effective way to evaluate the water status of plants and soil, and it can be used to monitor and regulate the soil water content, which can promote the improvement of plant production efficiency and quality. Although the photosynthetic activity of plant leaves can be accurately measured using the traditional gas-exchange method (Jia *et al.* 2023, Tominaga and Kawamitsu 2024), its application to soil water regulation is often limited by factors such as a long measurement time or a small monitoring range. Therefore, how to quickly and accurately obtain photosynthesis traits of *A. chinensis* leaves has become a key issue in establishing efficient and accurate water control technology and is an indispensable part of the current development of intelligent agriculture. This is important to improve the yield and quality of *A. chinensis*.

Hyperspectral reflectance technology has rich spectral information and good timeliness, which can accurately reflect the growth status and physiological characteristics of plants under different growth conditions nondestructively and in real time (Munné-Bosch and Villadangos 2023). It has been widely used in monitoring plant growth, agricultural production, and decision-making processes (Estrada *et al.* 2023, Flynn *et al.* 2024). Studies have shown that the leaf reflectance spectrum can diagnose nitrogen, phosphorus, or potassium deficiency in *Lactuca sativa* L. (Kanash *et al.* 2023), and monitor the drought tolerance of *Withania somnifera* (L.) Dunal (Singh 2023), cultivated soybeans (Poudel *et al.* 2023), and wheat (Rusakov and Kanash 2022, Ejaz *et al.* 2023), and reflect photosynthetic traits (Buchaillot *et al.* 2022) or metabolic responses (Burnett *et al.* 2021) under different conditions. However, the leaf reflectance spectrum is influenced by several factors, including structural factors, such as leaf thickness, dry matter, and water content, as well as physiological factors such as pigment concentration (Raypah *et al.* 2024). The changes observed in this spectrum under different water conditions are complex and exhibit a certain degree of inherent coupling. Its structural changes result in varied spectral characteristics and sensitivity of vegetation indices depending on plant species. Therefore, it is necessary to establish or verify the relationship between the reflectance spectrum and the leaf photosynthetic index for different plants.

In summary, to verify the feasibility of establishing precise water control technology for *A. chinensis* by using hyperspectral reflectance technology, we have analyzed the response of reflectance spectrum and photosynthetic activity of *A. chinensis* leaves to soil water content with a pot water control experiment and demonstrated the relationship between reflectance spectrum and photosynthetic activity in *A. chinensis* leaves. It can provide a theoretical basis and support establishing precise water control technology based on hyperspectral reflectance, promote the development of intelligent agriculture, and improve the quality of cultivated *A. chinensis*.

Materials and methods

Experimental materials and treatment: The annual *A. chinensis* seedlings with consistent growth and good development were provided by Chengde Bijiashan Ecological Agriculture Technology Development Co., Ltd., and taken as experimental materials in the autumn of 2023. Planting soil was taken from the cultivated layer (0–20 cm) of farmland, dried naturally, cleaned of impurities, and passed through a 6-mm pore size sieve, with a bulk density of 1.58 g cm^{-3}, pH 7.7, organic matter content of 3.46 g kg^{-1}, available nitrogen content of 62.6 mg kg^{-1}, available phosphorus content of 20.3 mg kg^{-1}, and available potassium content of 112.2 mg kg^{-1}. The selected seedlings of *A. chinensis* were transplanted into flowerpots (35 cm in diameter and 45 cm in height); each pot was filled with 4 kg of soil, and one seedling was transplanted. A total of 24 pots were transplanted and subjected to thorough watering and cultivation within a greenhouse environment [temperature: 20–25°C, irradiance: 0–600 μmol(photon) m^{-2} s^{-1}]. Growth environment conditions were maintained at a constant level throughout the culture period. To avoid obvious changes in soil water content, the soil was artificially weighed and rehydrated every 2 d. At the flowering stage, the plants with uniform growth were randomly divided into a control group (CTG) and a water consumption group (MCG), with 12 pots allocated to each treatment. The MCG was subjected to natural water depletion to create a multistage soil water gradient. The CTG

was maintained using the artificial water replenishment method maintaining the soil water content. Reflectance spectra, gas exchange, chlorophyll (Chl) *a* fluorescence of fully developed leaves, and the mass of the pot were then measured on 0, 2, 4, 6, and 10 d (denoted D_0, D_2, D_4, D_6, and D_{10}, respectively). Then the soil water content was calculated as follows: soil water content [%] = $(W_w - D_w)/D_w \times 100$, where W_w is the wet mass, and D_w is the dry mass.

Spectral reflectance: The spectral reflectance of the leaves was measured *in situ* using a *Unispec-SC* spectrometer (*PP Systems*, USA). The leaf illumination was provided by a tungsten halogen lamp in the spectrometer. The fully developed leaves from six pots of plants were selected for each treatment, and four different sites were determined for each leaf. Thereafter, the vegetation indexes used to measure water status, pigment content, and photosynthetic characteristics of the leaves were calculated according to Appendix 1. The average of the results was then calculated.

Gas exchange: The photosynthetic rate (P_N), the stomatal conductance (g_s), the transpiration rate (E), and the intercellular CO_2 concentration (C_i) of the leaves were measured *in situ* using a *CIRAS-4* portable photosynthesis measurement system (*PP Systems*, USA). The atmospheric conditions in the leaf chamber were controlled during the measurement, the PPFD was set at 1,200 μmol m^{-1} s^{-1}, the temperature was set at 25°C, and the CO_2 concentration was set at 360 μmol mol^{-1}. The light was provided by a red/blue LED source. The final mean value of P_N, g_s, E, and C_i was calculated from the fully developed leaves of six plants from each treatment. Then, the water-use efficiency (WUE) was calculated as P_N/E.

Chlorophyll *a* fluorescence: The fast Chl *a* fluorescence induction kinetics curve (OJIP curve) was measured *in situ* using a *Handy PEA* fluorescence meter (*Hansatech*, UK). The leaves were dark-adapted for 20 min, then induced by pulsed light at 3,000 μmol(photon) m^{-2} s^{-1}, and fluorescence signals from 10 μs to 1s were recorded. The OJIP curve was measured in the fully developed leaves of ten pots of plants from each treatment, and the results were averaged. The OJIP curve yielded several additional phenomenological and biophysical expressions facilitating structural and functional information regarding PSII. The selected parameters (Appendix 2) enabled the quantification and comparison of the PSII behavior observed in *A. chinensis* plants subjected to progressive water stress (Tsimilli-Michael 2020, Xue *et al.* 2022).

Statistical analysis: One-way analysis of variance (*ANOVA*) was used to assess all the data for obvious differences (P<0.05) by *SPSS 22.0* statistical software. The *Python 3.9* was used to construct graphs.

Results

Soil water content: The soil water content of the CTG was maintained within the range of 13.5–16.7% using artificial weighing of water replenishment throughout the experiment. In contrast, the soil water content of the MCG exhibited a gradual decline. The extension of the treatment time resulted in a multistage soil water gradient over time, with the lowest level observed on the 10th day, at 5.8%. This represents a 59.7% decrease compared to the control group (Fig. 1).

Leaf spectral reflectance: The spectral reflectance of plant leaves is influenced by multiple factors, such as leaf pigment content, water content, and physiological, and biochemical conditions. Alterations in the growth environment consequently result in changes in the reflectance characteristics. The reflectance of the leaves of *A. chinensis* exhibited a gradual increase with the progression of treatment time in the near-infrared band (740–1,000 nm). Conversely, the visible band (450–680 nm) significantly increased at D_{10} (Fig. 2*B*). In contrast, there was no significant change in the spectral reflectance of *A. chinensis* leaves in CTG (Fig. 2*A*). Meanwhile, the vegetation indices PRI and $PSSR_b$, which reflect leaf photosynthetic activity and Chl *b* content, demonstrated a decline with decreasing soil water content in MCG. Conversely, the indices NWI and WI, which reflect leaf water status, exhibited a gradual increase. In contrast, the index $PSSR_a$ remained unchanged. This demonstrated minimal fluctuations in the CTG (Table 1).

Gas-exchange parameters: As illustrated in Fig. 3, the P_N, g_s, E, C_i, and WUE in the leaves of *A. chinensis* plants grown in the CTG treatment remained relatively stable due to the soil water content being maintained at a normal level. However, the reduction in soil water content in MCG resulting from natural water consumption led to notable alterations in the gas-exchange parameters of *A. chinensis* leaves. A significant decrease in the values of P_N, g_s, and E was observed in association with a reduction in soil water content, with values of 0.85 μmol m^{-2} s^{-1}, 23.88 mol m^{-2} s^{-1}, and 0.62 mol m^{-2} s^{-1} on day 10, which were 93.9, 94.1, and 86.4% lower than the control,

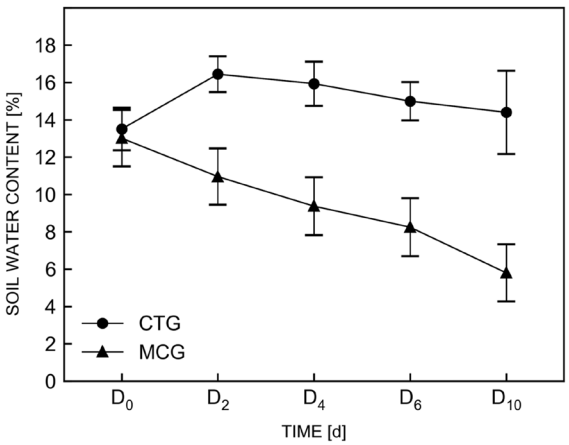

Fig. 1. Changes in soil water content in CTG and MCG. CTG – control group; MCG – water consumption group. Values are means ± SDs (n = 12).

respectively. Nevertheless, the data indicated a pattern of initial decline followed by an increase in C_i, while WUE demonstrated an initial increase followed by a decline.

Chlorophyll *a* fluorescence: The Chl *a* fluorescence induction curve (OJIP curve) contains a great deal of information about primary photochemical reactions and has been widely used to monitor changes in the photosynthetic apparatus of plants under different conditions (Tsimilli-Michael 2020). This study demonstrated no significant alteration in the OJIP curve in the *A. chinensis* leaves of CTG when soil water content was maintained at a normal level (Fig. 4*A*). Nevertheless, the OJIP curve of MCG exhibited a pronounced change in its shape in response to variations in soil water content, with the degree of alteration being most pronounced at D_{10} (Fig. 4*B*). This result indicates that the alteration in soil water content influenced the photosynthetic primary reaction of electron transfer chain in *A. chinensis* leaves. The quantitative analysis of the OJIP curve indicated that the fluorescence parameters V_J, V_I, ABS/RC, TR_0/RC, and DI_0/RC in *A. chinensis* leaves from MCG exhibited an increasing trend, PI_{ABS} and PI_{total} decreased significantly, and the other parameters (φ_{P0}, ψ_{E0}, δ_{R0}, ET_0/RC, RE_0/RC) did not change significantly with decreasing soil water content (Fig. 5*B*). Additionally, there was no discernible change in the fluorescence parameters in *A. chinensis* leaves from CTG (Fig. 5*A*).

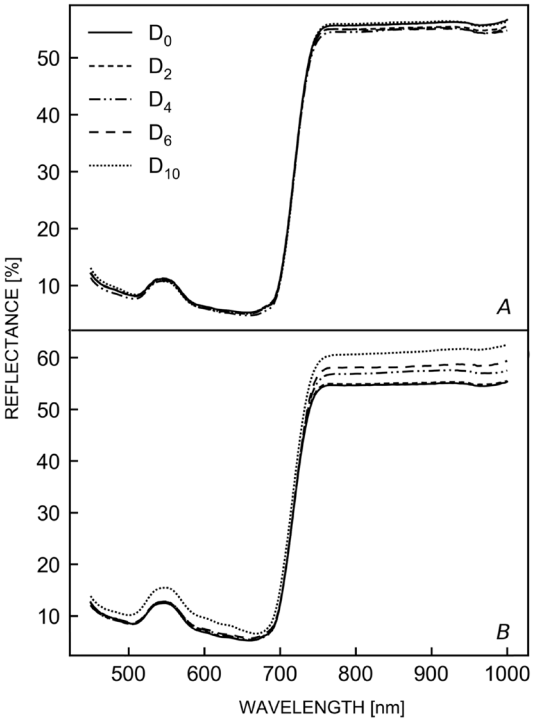

Fig. 2. Response of spectral reflectance in *Atractylodes chinensis* leaves to different soil water content treatments of CTG (*A*) and MCG (*B*). Twenty-four measurements were made for each treatment and the results were averaged. CTG – control group; MCG – water consumption group.

Relationship between leaf vegetation indices and photosynthetic activity: To gain a deeper insight into the relationship between leaf reflectance spectral vegetation indices and the photosynthetic activity of *A. chinensis* under varying soil water gradients, a correlation analysis was conducted between leaf vegetation indices and typical photosynthetic characteristics under different soil water contents (n = 10). The results demonstrated a significant correlation between vegetation indices including PRI, $PSSR_b$, NWI, and WI with photosynthetic activity indices P_N, g_s, E, PI_{ABS}, and PI_{total} under varying soil water gradients (Fig. 6).

Discussion

Photosynthesis, as an important indicator of the physiological state of plants, can respond quickly to changes in soil water content (Gupta *et al.* 2020, Ilyas *et al.* 2021). Among these, P_N is frequently employed as a crucial physiological indicator to delineate the response of plants to soil water content (Tankari *et al.* 2021, Nión *et al.*

Table 1. Response of vegetable indices PRI, $PSSR_a$, $PSSR_b$, NWI, and WI in *Atractylodes chinensis* leaves to different soil water content. The mean ± SE values of twenty-four replicates are shown. *Different lowercase letters* in a column represent obvious differences at $P<0.05$ level. NWI – normalized difference water index; PRI – photochemical reflection index; $PSSR_a$ – pigment specific simple ratio of chlorophyll *a*; $PSSR_b$ – pigment specific simple ratio of chlorophyll *b*; WI – water index; CTG – control group; MCG – water consumption group.

Treatment	Time (day)	PRI	$PSSR_a$	$PSSR_b$	NWI	WI
CTG	D_0	0.09 ± 0.01^a	9.04 ± 0.69^a	10.09 ± 1.10^a	–0.003 ± 0.006^c	0.99 ± 0.01^b
	D_2	0.09 ± 0.01^a	8.77 ± 0.66^a	9.99 ± 1.10^a	–0.005 ± 0.002^c	0.99 ± 0.00^b
	D_4	0.08 ± 0.01^a	9.96 ± 0.87^a	10.73 ± 1.22^a	–0.007 ± 0.002^c	0.99 ± 0.00^b
	D_6	0.09 ± 0.01^a	9.08 ± 0.80^a	10.35 ± 1.25^a	–0.007 ± 0.004^c	0.99 ± 0.01^b
	D_{10}	0.10 ± 0.01^a	9.22 ± 0.51^a	10.47 ± 0.86^a	–0.007 ± 0.003^c	0.99 ± 0.01^b
MCG	D_0	0.08 ± 0.01^a	8.86 ± 0.47^a	9.48 ± 0.55^a	–0.004 ± 0.001^c	0.99 ± 0.00^b
	D_2	0.08 ± 0.01^a	9.71 ± 0.47^a	9.42 ± 0.70^{ab}	–0.003 ± 0.002^c	0.99 ± 0.00^b
	D_4	0.07 ± 0.01^b	9.49 ± 0.70^a	9.34 ± 0.72^b	–0.004 ± 0.002^c	0.99 ± 0.01^b
	D_6	0.07 ± 0.00^b	9.08 ± 0.37^a	9.15 ± 0.44^c	–0.001 ± 0.004^b	1.00 ± 0.01^a
	D_{10}	0.06 ± 0.02^c	8.53 ± 0.66^b	7.81 ± 1.52^d	0.002 ± 0.004^a	1.00 ± 0.00^a

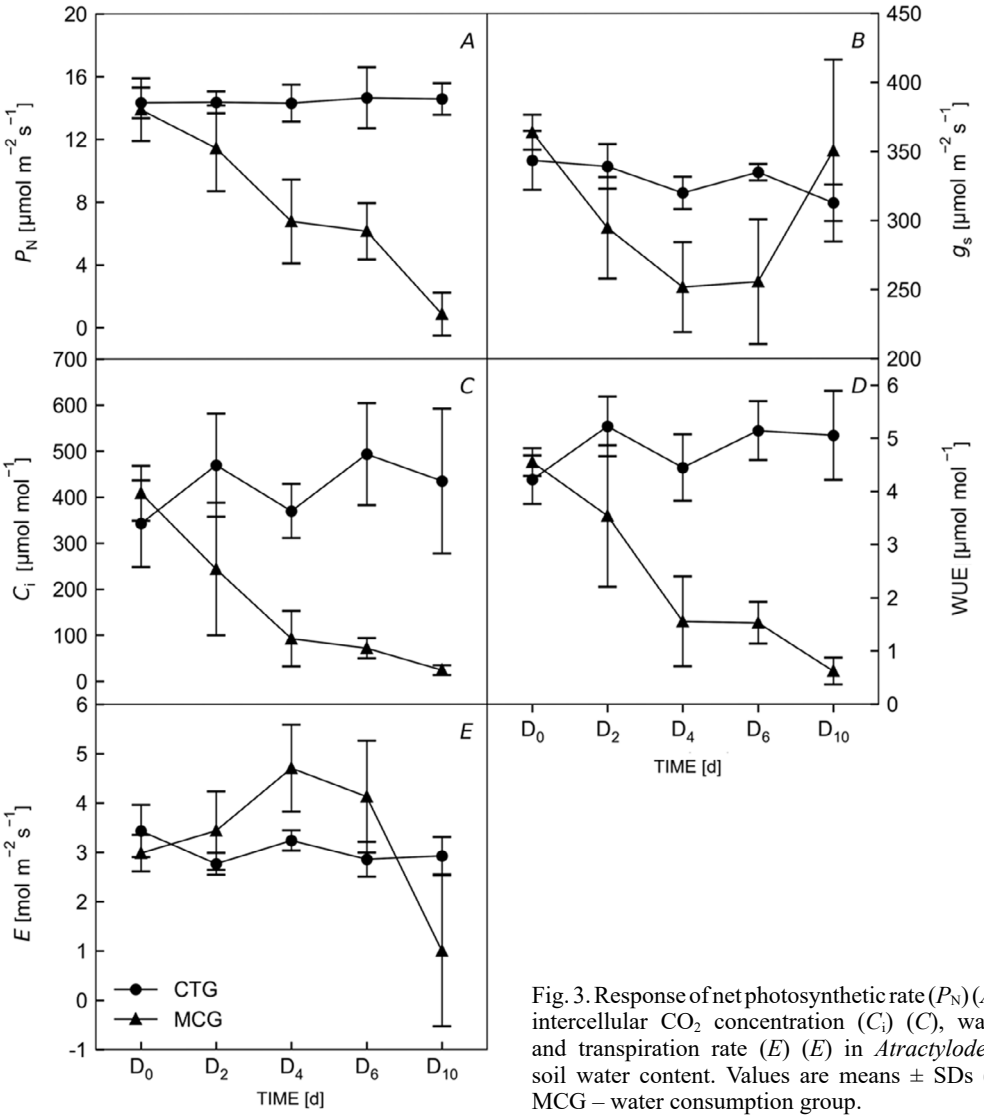

Fig. 3. Response of net photosynthetic rate (P_N) (*A*), stomatal conductance (g_s) (*B*), intercellular CO_2 concentration (C_i) (*C*), water-use efficiency (WUE) (*D*), and transpiration rate (*E*) (*E*) in *Atractylodes chinensis* leaves to different soil water content. Values are means ± SDs (n = 6). CTG – control group; MCG – water consumption group.

2024). In this study, the P_N and WUE in *A. chinensis* leaves of CTG remained relatively stable when the soil water content was within the 13.5–16.7% range. Conversely, the P_N decreased while WUE increased significantly as soil water content initially decreased in the MCG group. The observed trend was attributed to the fact that ABA, which is produced in the roots in response to declining soil water content, induced stomatal closure, leading to a reduction in g_s and E (Lima *et al.* 2021). However, as soil water content further decreased to 5.8–8.2%, the P_N and WUE of *A. chinensis* leaves declined, C_i increased significantly, which indicate a shift in the limiting factors of photosynthesis from primarily stomatal to nonstomatal restrictions at this stage. The causes underlying the reduction in photosynthesis in *A. chinensis* leaves are inversely correlated with soil water content, exhibiting a similar response pattern to that observed in maize under soil water stress (Jia *et al.* 2020). Previous studies have demonstrated that the stomatal turning point of photosynthesis is the lowest water deficit for plants to maintain normal growth. Beyond this threshold, if water stress persists, plants experience a severe reduction in their photosynthetic productivity.

Inhibition of photosynthetic carbon assimilation reduces the consumption of ATP and NADPH, leading to feedback inhibition of photosynthetic electron transfer in chloroplasts (Xue *et al.* 2014). In this study, we used the technique of Chl *a* fluorescence to reflect the state of the photosynthetic electron transport (Li *et al.* 2019, Rapacz *et al.* 2019). The results showed that the photosynthetic electron transfer process of *A. chinensis* leaves in the MCG was strongly inhibited as the water content of the soil decreased to 5.8% on the 10th day, which was proven by the significant change of OJIP curves. There was a gradual increase in V_J and V_I as a result of natural water consumption, which indicated a limited electron transfer after Q_A and PQH_2. The inhibition of electron transport has been demonstrated to increase the likelihood of generating reactive oxygen species (ROS), which in turn has the potential to cause membrane damage and the deterioration of membrane integrity. The dramatically decreased PI_{total}, which has the four main structural and

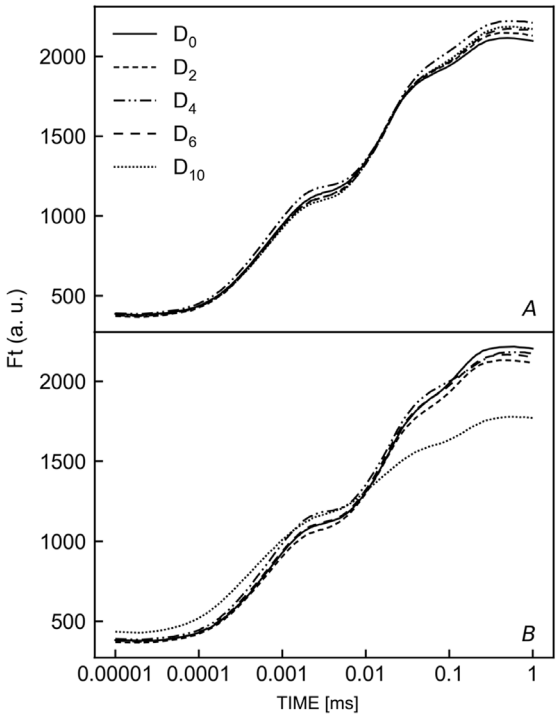

Fig. 4. Response of chlorophyll *a* fluorescence in *Atractylodes chinensis* leaves to different soil water content treatments of CTG (*A*) and MCG (*B*). Ten replicates were made for each treatment and results averaged. F_t – fluorescence emission from a dark-adapted leaf at the time t; CTG – control group; MCG – water consumption group.

functional parameters, including ABS/RC, φ_{P0}, ψ_{E0}, and δ_{R0}, indicates that the ability of energy conservation and the activity of photosynthetic apparatus were inhibited by the decreasing soil water content and suggests that the damage of photosynthetic apparatus was one of the reasons of decreased P_N under severe soil water content. The reduction in RC/CS_0 indicates a decline in the number of functional reaction centers, which increases the energy absorbed and transferred by each reaction center, as well as an increase in ABS/RC and TR_0/RC. Thus, the apparent rise in DI_0/RC in *A. chinensis* leaves in the MCG was a dissipation of excess excitation energy. Then, the photosynthetic apparatus of *A. chinensis* leaves was irreversibly disrupted as a consequence of the generation of ROS due to the absence of timely energy dissipation. Guha *et al.* (2013) demonstrated using Chl *a* fluorescence and proteomic analysis techniques that mulberry trees can comprehensively downregulate the photosynthetic process without serious damage to the structural and functional integrity of PSII under prolonged drought conditions to maintain the internal balance between electron transfer reaction and reduction of carbon metabolism. Our study demonstrated that the nonstomatal limitation factors of photosynthesis in *A. chinensis* leaves can be partially attributed to the destruction of the photosynthetic apparatus. However, it has long been recognized that ROS serve as a fundamental factor in inducing increased secondary metabolism. In essence, ROS activate gene expression and alter enzyme structures, thereby enhancing the activity of key rate-limiting enzymes essential for producing secondary metabolites (Borges *et al.* 2017).

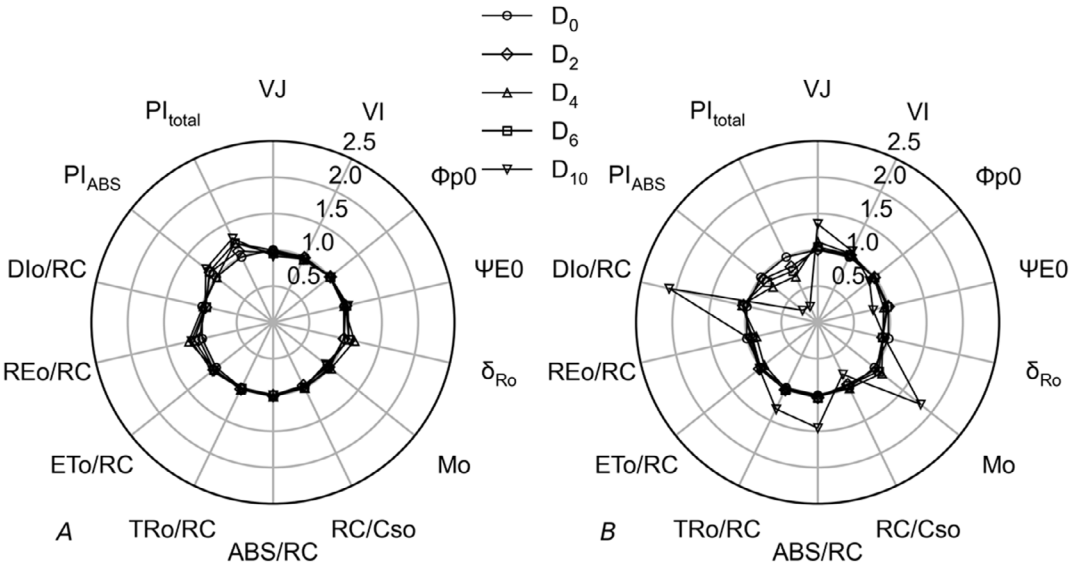

Fig. 5. Response of chlorophyll *a* fluorescence parameters in *Atractylodes chinensis* leaves to different soil water content of CTG (*A*) and MCG (*B*). Ten measurements were taken for each treatment, after which the average result was calculated. ABS/RC – absorption flux per RC; DI_0/RC – dissipated energy flux per RC at t = 0; ET_0/RC – electron transport flux per RC at t = 0; M_0 – slope of the curve at the origin of the relative variable fluorescence rise; PI_{ABS} – performance index; PI_{total} – the total performance index; RC/CS_0 – Q_A^- reducing RCs per CS; RE_0/RC – electron flux per active RC reducing the end electron acceptors on the acceptor side of PSI at t = 0; TR_0/RC – trapped energy flux per RC at t = 0; δ_{R0} – probability that an electron is transported from the reduced intersystem electron acceptors to the final electron acceptors of PSI; φ_{P0} – maximum quantum yield for primary photochemistry; ψ_{E0} – probability that an electron moves further than Q_A^-.

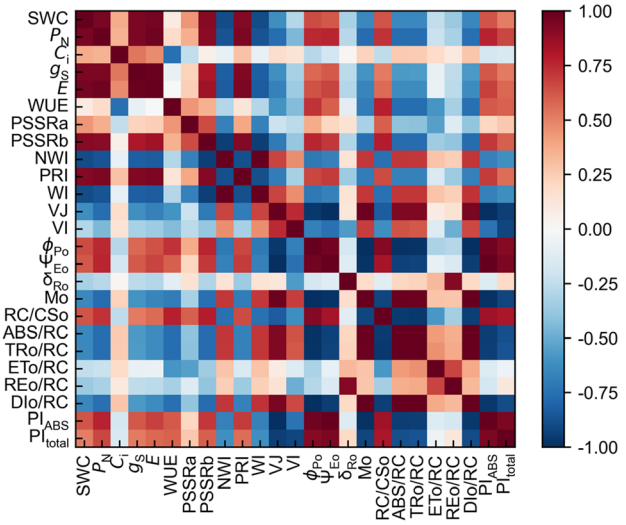

Fig. 6. Relationship between leaf vegetation indices and photosynthetic activity of *Atractylodes chinensis* leaves under different soil water content. ABS/RC – absorption flux per RC; C_i – intercellular CO_2 concentration; CTG – control group; DI_0/RC – dissipated energy flux per RC at t = 0; *E* – transpiration rate; ET_0/RC – electron transport flux per RC at t = 0; F_t – fluorescence emission from a dark-adapted leaf at the time t; g_s – stomatal conductance; MCG – water consumption group; M_0 – slope of the curve at the origin of the relative variable fluorescence rise; NWI – normalized difference water index; PI_{ABS} – performance index; PI_{total} – the total performance index; P_N – net photosynthetic rate; PRI – photochemical reflection index; $PSSR_a$ – pigment specific simple ratio of chlorophyll *a*; $PSSR_b$ – pigment specific simple ratio of chlorophyll *b*; RC/CS_0 – Q_A^- reducing RCs per CS; RE_0/RC – electron flux per active RC reducing the end electron acceptors on the acceptor side of PSI at t = 0; TR_0/RC – trapped energy flux per RC at t = 0; WI – water index; WUE – water-use efficiency; δ_{R0} – probability that an electron is transported from the reduced intersystem electron acceptors to the final electron acceptors of PSI; φ_{P0} – maximum quantum yield for primary photochemistry; ψ_{E0} – probability that an electron moves further than Q_A^-.

Consequently, a moderate degree of water stress will be conducive to the synthesis and accumulation of the medicinal components of *A. chinensis*. Based on the above analysis, the gas exchange or Chl *a* fluorescence technique can accurately reflect the photosynthetic activity of *A. chinensis* at different soil water contents.

Hyperspectral reflectance technology has the characteristics of rich spectral information and good timeliness, which timely reflect physiological indices, such as water status, pigment content, nutrient status, and photosynthetic fluorescence of plants and their internal correlation (Singh 2023, Raypah *et al.* 2024). Water is an important component of leaves, so the lack of water can cause their physiological changes. It is the foundation for monitoring physiological and water status using hyperspectral reflectance techniques. In the present study, the spectral reflectance of *A. chinensis* leaves increased with reduced soil water content in the visible (450–680 nm) and near-infrared (740–1,000 nm) bands, but the variation was more marked in the near-infrared band. The vegetable indices WI and NWI, which are derived from the spectral reflectance, have been used to reflect the water content of leaves (Penuelas *et al.* 1997, Blackburn 1998). Thus, WI and NWI increased with decreasing soil water content in this study, demonstrating that the water content of *A. chinensis* leaves decreased gradually. Studies have shown that $PSSR_a$ and $PSSR_b$ can reflect the content of Chl *a* and *b* in the leaves (Blackburn 1998), which are involved in the absorption, transfer, and transformation of light energy in plant photosynthesis. However, $PSSR_a$ showed no obvious changes, while $PSSR_b$ decreased gradually with decreasing soil water content in this study. The ROS generated by the blocked photosynthetic electron transfer led to the degradation of Chl *b*, which is more susceptible to the effects than Chl *a*. The PRI has been demonstrated to exhibit a strong correlation with the pigment content related to the lutein cycle in plant leaves. This correlation reflects the photosynthetic rate and light energy-use efficiency of plants. Furthermore, it demonstrates a declining trend with reducing soil water content. Its correlation with P_N and PI_{total} is also noteworthy, aligning with previous research findings (Kalisz *et al.* 2023, Song *et al.* 2023). It can be concluded from the above that spectral reflectance can be employed to monitor and evaluate the photosynthetic activity of *A. chinensis* leaves under different soil water conditions. This has the potential to be applied in the field of water regulation.

Conclusions: The relationship between vegetable indices and photosynthetic characteristics under varying soil water content provides insights into the utility of spectral reflectance as an effective tool to assess changes in the photosynthetic activity of leaves of *A. chinensis* in response to water deficits. The technology has the potential to be widely applicable in the monitoring of drought conditions and the regulation of soil water in the cultivation of *A. chinensis*. However, this study did not consider the impact of water control at different growth stages on the photosynthetic activity of *A. chinensis* leaves, nor was there a sufficient body of research available at the population, canopy, and ecological levels. These limitations will be addressed in future studies.

References

Asgari A., Hooshmand A., Broumand-Nasab S., Zivdar S.: Potential application of spectral indices for olive water status assessment in (semi-)arid regions: A case study in Khuzestan Province, Iran. – Plant Direct **7**: e494, 2023.

Blackburn G.A.: Quantifying chlorophylls and caroteniods at leaf and canopy scales: An evaluation of some hyperspectral approaches. – Remote Sens. Environ. **66**: 273-285, 1998.

Borges C.V., Minatel I.O., Gomez-Gomez H.A., Lima G.P.P.: Medicinal plants: Influence of environmental factors on the content of secondary metabolites. – In: Ghorbanpour M., Varma A. (ed.): Medicinal Plants and Environmental Challenges. Pp. 259-277. Springer, Cham 2017.

Buchaillot M.L., Soba D., Shu T. *et al.*: Estimating peanut and soybean photosynthetic traits using leaf spectral reflectance and advance regression models. – Planta **255**: 93, 2022.

Burnett A.C., Serbin S.P., Davidson K.J. *et al.*: Detection of the metabolic response to drought stress using hyperspectral reflectance. – J. Exp. Bot. **72**: 6474-6489, 2021.

Ejaz I., Li W., Naseer M.A. *et al.*: Detection of combined

frost and drought stress in wheat using hyperspectral and chlorophyll fluorescence imaging. – Environ. Technol. Innov. **30**: 103051, 2023.

Estrada F., Flexas J., Araus J.L. *et al.*: Exploring plant responses to abiotic stress by contrasting spectral signature changes. – Front. Plant Sci. **13**: 1026323, 2023.

Flynn K.C., Witt T.W., Baath G.S. *et al.*: Hyperspectral reflectance and machine learning for multi-site monitoring of cotton growth. – Smart Agric. Technol. **9**: 100536, 2024.

Gamon J.A., Peñuelas J., Field C.B.: A narrow-waveband spectral index that tracks diurnal changes in photosynthetic efficiency. – Remote Sens. Environ. **41**: 35-44, 1992.

Guha A., Sengupta D., Reddy A.R.: Polyphasic chlorophyll *a* fluorescence kinetics and leaf protein analyses to track dynamics of photosynthetic performance in mulberry during progressive drought. – J. Photoch. Photobio. B **119**: 71-83, 2013.

Gupta A., Rico-Medina A., Caño-Delgado A.I.: The physiology of plant responses to drought. – Science **368**: 266-269, 2020.

Ilyas M., Nisar M., Khan N. *et al.*: Drought tolerance strategies in plants: A mechanistic approach. – J. Plant Growth Regul. **40**: 926-944, 2021.

Jia Q., Liu Z., Guo C. *et al.*: Relationship between photosynthetic CO_2 assimilation and chlorophyll fluorescence for winter wheat under water stress. – Plants-Basel **12**: 3365, 2023.

Jia Y., Xiao W., Ye Y. *et al.*: Response of photosynthetic performance to drough duration and re-watering in maize. – Agronomy **10**: 533, 2020.

Kalisz A., Kornaś A., Skoczowski A. *et al.*: Leaf chlorophyll fluorescence and reflectance of oakleaf lettuce exposed to metal and metal(oid) oxide nanoparticles. – BMC Plant Biol. **23**: 329, 2023.

Kanash E.V., Sinyavina N.G., Rusakov D.V. *et al.*: Morpho-physiological, chlorophyll fluorescence, and diffuse reflectance spectra characteristics of lettuce under the main macronutrient deficiency. – Horticulturae **9**: 1185, 2023.

Lei H., Yue J., Yin X. *et al.*: HS-SPME coupled with GC–MS for elucidating differences between the volatile components in wild and cultivated *Atractylodes chinensis*. – Phytochem. Analysis **34**: 317-328, 2023.

Lei J., Tu Y., Xu J., Yu J.: Mechanisms of the traditional Chinese herb *Atractylodes lancea* against COVID-19 based on network pharmacology and molecular docking. – Wuhan Univ. J. Nat. Sci. **27**: 349-360, 2022.

Li Y., Song H., Zhou L. *et al.*: Tracking chlorophyll fluorescence as an indicator of drought and rewatering across the entire leaf lifespan in a maize field. – Agr. Water Manage. **211**: 190-201, 2019.

Lima A.A., Santos I.S., Torres M.E.L. *et al.*: Drought and re-watering modify ethylene production and sensitivity, and are associated with coffee anthesis. – Environ. Exp. Bot. **181**: 104289, 2021.

Ma S., Sun C., Su W. *et al.*: Transcriptomic and physiological analysis of *Atractylodes chinensis* in response to drought stress reveals the putative genes related to sesquiterpenoid biosynthesis. – BMC Plant Biol. **24**: 91, 2024.

Ma Z., Liu G., Yang Z. *et al.*: Species differentiation and quality evaluation for *Atractylodes* medicinal plants by GC/MS coupled with chemometric analysis. – Chem. Biodivers. **20**: e202300793, 2023.

Munné-Bosch S., Villadangos S.: Cheap, cost-effective, and quick stress biomarkers for drought stress detection and monitoring in plants. – Trends Plant Sci. **28**: 527-536, 2023.

Nión M., Gándara J., Ross S. *et al.*: Photosynthesis adaptation to long- and short-term water restriction in commercial plantlets of *Eucalyptus grandis* and hybrids with Red Gums. – Trees **38**: 537-547, 2024.

Penuelas J., Pinol J., Ogaya R., Filella I.: Estimation of plant water concentration by the reflectance Water Index WI (R900/R970). – Int. J. Remote Sens **18**: 2869-2875, 1997.

Poudel S., Vennam R.R., Shrestha A. *et al.*: Resilience of soybean cultivars to drought stress during flowering and early-seed setting stages. – Sci. Rep.-UK **13**: 1277, 2023.

Rapacz M., Wójcik-Jagła M., Fiust A. *et al.*: Genome-wide associations of chlorophyll fluorescence OJIP transient parameters connected with soil drought response in barley. – Front. Plant Sci. **10**: 78, 2019.

Raypah M. E., Nasru M.I.M., Nazim M.H.H. *et al.*: Reflectance spectra for identifying stress in different parts of leaf: a case study on oil palm seedlings. – Int. J. Remote Sens. **45**: 954-980, 2024.

Rusakov D.V., Kanash E.V.: Spectral characteristics of leaves diffuse reflection in conditions of soil drought: a study of soft spring wheat cultivars of different drought resistance. – Plant Soil Environ. **68**: 137-145, 2022.

Singh R.: Spectral reflectance and fluorescence is a rapid, non-destructive tool for drought tolerance monitoring in *Withania somnifera* (L.) Dunal. – Protoplasma **260**: 1421-1435, 2023.

Song K.E., Hong S.S., Hwang H.R. *et al.*: Effect analysis of hydrogen peroxide using hyperspectral reflectance in sorghum [*Sorghum bicolor* (L.) Moench] under drought stress. – Plants-Basel **12**: 2958, 2023.

Tankari M., Wang C., Ma H. *et al.*: Drought priming improved water status, photosynthesis and water productivity of cowpea during post-anthesis drought stress. – Agr. Water Manage. **245**: 106565, 2021.

Tominaga J., Kawamitsu Y.: Combined leaf gas-exchange system for model assessment. – J. Exp. Bot. **75**: 2982-2993, 2024.

Tsimilli-Michael M.: Revisiting JIP-test: An educative review on concepts, assumptions, approximations, definitions and terminology. – Photosynthetica **58**: 275-292, 2020.

Wang Y., Xue Z., Yang Y. *et al.*: [Effects of climate change on the distribution pattern of the suitable growing region for *Atractylodes chinensis* (DC.) Koidz. in Yanshan area.] – Chin. J. Inform. Tradit. Chin. Med. **30**: 1-7, 2023. [In Chinese]

Xia Y.-G., Yang B.-Y., Wang Q.-H. *et al.*: Species classification and quality assessment of Cangzhu (Atractylodis Rhizoma) by high-performance liquid chromatography and chemometric methods. – J. Anal. Methods Chem. **2013**: 497532, 2013.

Xu J., Chen D., Liu C. *et al.*: Structural characterization and anti-tumor effects of an inulin-type fructan from *Atractylodes chinensis*. – Int. J. Biol. Macromol. **82**: 765-771, 2016.

Xue Z., Gao H., Zhao S.: Effects of cadmium on the photosynthetic activity in mature and young leaves of soybean plants. – Environ. Sci. Pollut. Res. **21**: 4656-4664, 2014.

Xue Z.C., Wang Y., Liu J.: Systematic salt tolerance-related physiological mechanisms of wild soybean and their role in the photosynthetic activity and Na^+ distribution of grafted soybean plants. – Photosynthetica **60**: 400-407, 2022.

Zhang A., Liu M., Gu W. *et al.*: Effect of drought on photosynthesis, total antioxidant capacity, bioactive component accumulation, and the transcriptome of *Atractylodes lancea*. – BMC Plant Biol. **21**: 293, 2021b.

Zhang W., Bai Q., Cui G. *et al.*: Recent progress and ongoing challenges in Rhizoma atractylodis research: biogeography, biosynthesis, quality formation and control. – Med. Plant Biol. **2**: 19, 2023.

Zhang W., Zhao Z., Chang L. *et al.*: Atractylodis Rhizoma: A review of its traditional uses, phytochemistry, pharmacology, toxicology and quality control. – J. Ethnopharmacol. **266**: 113415, 2021a.

Appendix 1. The equation of vegetation indices deriving from spectral reflectance. R_X is the spectral reflectance at X wavelength.

Vegetation index	Abbreviation	Equation	Reference
Photochemical reflection index	PRI	$PRI = (R_{531} - R_{570})/(R_{531} + R_{570})$	Gamon *et al.* (1992)
Pigment-specific simple ratio (Chl *a*)	$PSSR_a$	$PSSR_a = R_{800}/R_{680}$	Blackburn (1998)
Pigment-specific simple ratio (Chl *b*)	$PSSR_b$	$PSSR_b = R_{800}/R_{635}$	Blackburn (1998)
Water index	WI	$WI = R_{970}/R_{900}$	Penuelas *et al.* (1997)
Normalized difference water index	NWI	$NWI = (R_{970} - R_{900})/(R_{970} + R_{900})$	Asgari *et al.* (2023)

Appendix 2. The selection of JIP-test parameters and the equations used in this study.

Parameter	Description	Equation
F_t	Fluorescence emission from a dark-adapted leaf at the time t	
M_0	The slope of the curve at the origin of the relative variable fluorescence rise	$M_0 = 4(F_{300\mu s} - F_0)/(F_m - F_0)$
φ_{P0}	Maximum quantum yield for primary photochemistry	$\varphi_{P0} = (F_m - F_0)/F_m$
ψ_{E0}	The probability that an electron moves further than Q_A^-	$\psi_{E0} = 1 - V_J$
δ_{R0}	Probability that an electron is transported from the reduced intersystem electron acceptors to the final electron acceptors of PSI	$\delta_{R0} = (1 - V_I)/(1 - V_J)$
RC/CS_0	Q_A^- reducing RCs per CS	$RC/CS_0 = \varphi_{P0}\ (ABS/CS_0)(V_J/M_0)$
ABS/RC	Absorption flux per RC	$ABS/RC = M_0\ (1/V_J)(1/\varphi_{P0})$
TR_0/RC	Trapped energy flux per RC at t = 0	$TR_0/RC = M_0/V_J$
ET_0/RC	Electron transport flux per RC at t = 0	$ET_0/RC = M_0(1/V_J)\ \psi_{E0}$
RE_0/RC	Electron flux per active RC reducing the end electron acceptors on the acceptor side of PSI at t = 0	$RE_0/RC = M_0(1/V_J)(1 - V_I)$
DI_0/RC	Dissipated energy flux per RC at t = 0	$DI_0/RC = ABS/RC - TR_0/RC$
PI_{ABS}	The performance index	$PI_{ABS} = (RC/ABS)[\varphi_{P0}/(1 - \varphi_{P0})][\psi_{E0}/(1 - \psi_{E0})]$
PI_{total}	The total performance index	$PI_{total} = PI_{ABS}\ [\delta_{R0}/(1 - \delta_{R0})]$